Journal of Pain Research

Dovepress
open access to scientific and medical research

Open Access Full Text Article

ORIGINAL RESEARCH

Restoration of the Activity of the Prefrontal Cortex to the Nucleus Accumbens Core Pathway Relieves Fentanyl-Induced Hyperalgesia in Male Rats

Qiong Luo[1,*], Jing Luo[1,*], Xixi Wang[2], Sifei Gan[3]

[1]Department of Anesthesiology, Zhongnan Hospital of Wuhan University, Wuhan, Hubei, People's Republic of China; [2]Department of Anesthesiology, Tongji Hospital, Tongji Medical College, Huazhong University of Science and Technology, Wuhan, Hubei, People's Republic of China; [3]Department of Anesthesiology, The First Hospital of Nanchang, Nanchang, Jiangxi, People's Republic of China

*These authors contributed equally to this work

Correspondence: Sifei Gan, Department of Anesthesiology, The First Hospital of Nanchang, Nanchang, Jiangxi, People's Republic of China, Email sifei1632023@163.com

Purpose: Functional connectivity between the prelimbic medial prefrontal cortex (PL-mPFC) and the core of the nucleus accumbens (NAc core) predicts pain chronification. Inhibiting the apoptosis of oligodendrocytes in the PL-mPFC prevents fentanyl-induced hyperalgesia in rats. However, the role of prefrontal cortex (PFC)-NAc projections in opioid-induced hyperalgesia (OIH) remains unclear. Herein, we explored the role of the PL-NAc core circuit in fentanyl-induced hyperalgesia.

Methods: An OIH rat model was established, and patch-clamp recording, immunofluorescence, optogenetics, and chemogenetic methods were employed for neuron excitability detection and nociceptive behavioral assessment.

Results: Our results showed decreased activity of the right PL-mPFC layer V output neurons in rats with OIH. Similarly, the excitability of the NAc core neurons receiving glutamatergic projections from the PL-mPFC decreased in OIH rats, observed by the light-evoked excitatory postsynaptic currents/light-excited inhibitory postsynaptic currents ratio (eEPSC/eIPSC ratio). Fentanyl-induced hyperalgesia was reversed by optogenetic activation of the PL-NAc core pathway, and chemogenetic suppression of this pathway induced hyperalgesia in control (saline-treated) rats. However, behavioral hyperalgesia was not aggravated by this chemogenetic suppression in OIH (fentanyl-treated) rats.

Conclusion: Our findings indicate that inactivation of the PL-NAc core pathway may be a cause of OIH and restoring the activity of this pathway may provide a strategy for OIH treatment.

Keywords: fentanyl-induced hyperalgesia, prelimbic medial prefrontal cortex, nucleus accumbens core, circuit

Introduction

Opioid-induced effects on the nociceptive system include a relative block in nociceptive transmission, system sensitization, and desensitization towards afferent nociception and opioid agonists, respectively. Corresponding effects include analgesia, opioid-induced hyperalgesia (OIH), and tolerance. OIH is a state of hypersensitivity caused by large opioid exposure that does not improve or even worsens with continuous opioid usage.[1] This paradoxical phenomenon has become a challenge in current clinical analgesic treatment, prompting an urgency for investigating the mechanism of its occurrence.

Several causes of OIH exist, however, it is speculated to begin primarily in the brain or brainstem before traveling through the spinal cord to the area of pain. Additionally, OIH is caused by dysfunction of the nociceptive pathway down the spinal cord through the rostral ventral medulla.[2] Activating neurons that project from the periaqueductal gray (PAG) to the rostral ventromedial medulla (RVM) and subsequently to the spinal cord is a common classic circuit of pain downward the control route.[3–5] The medial prefrontal cortex (mPFC) is involved in pain perception and sensation. Furthermore, it is implicated in the pain process, observed by its close projections to other brain regions such as PAG and nucleus accumbens (NAc).[6–8] The prefrontal cortex (PFC) neurons project to PAG at the circuit level, which provides

Received: 19 October 2023
Accepted: 11 March 2024
Published: 20 March 2024

output to the RVM to form a classic descending inhibitory circuit. However, activating projections from the PFC to the NAc, an important pathway in the brain's reward circuitry, can inhibit both the sensory and affective components of pain.[9] Clinical neuroimaging studies revealed that the functional connection of the mPFC-NAc is altered in the chronic pain state, indicating that pain sensitivity may be closely related to the cerebral cortex and reward circuit.[10] Moreover, excessive activation of PFC-NAc projections can alter pain phenotypes,[11] suggesting that the mPFC-NAc circuit plays a crucial role in pain regulation.

Anatomically, the mPFC can be classified into the anterior cingulate cortex (ACC), prelimbic cortex (PL) and infralimbic cortex (IL) subregions.[12] Among them, the PL is crucial for pain perception and has been widely studied. Decreased activity of prelimbic cortex is involved in the comorbidity of neuropathic pain and depression in rats.[13] Current literature suggests that different regions within the PFC play distinct roles in pain regulation. Both the PL and the ACC project to the NAc core at the circuit level, whereas the IL-PFC has a weaker input to the shell subregion of the NAc.[14] Our previous research revealed that inhibiting apoptosis of oligodendrocytes in the prelimbic medial prefrontal cortex (PL-mPFC) can prevent fentanyl-induced hyperalgesia in rats.[15] However, the definite role of PFC-NAc projections in OIH remains unclear. In this study, we aimed to investigate the role of the PL-NAc core circuit in fentanyl-induced hyperalgesia.

Materials and Methods

Animals

All experimental rats were purchased from the Biont Company (Wuhan, China). Male Sprague–Dawley rats weighing 60–280 g were housed in a temperature-controlled space with a 12 h light/dark cycle and free access to food and water. All the experiments were conducted only on male rats.[16,17] All animals were acclimated to the environment for 3 days before the experiments were carried out. Rats were 4 weeks old, weighing 60–70 g initially before being administered the viral vector injection. Brain slice physiology and behavioral assays were conducted 3–4 weeks after the viral vector injection. This study was conducted in accordance with the National Institutes of Health Guidelines for the Care and Use of Laboratory Animals and was approved by the Laboratory Animal and Biomedical Ethics Committee of the South-Central University for Nationalities (Number: 2019- SCUEC-AEC-022).

OIH Model

The OIH modeling method was previously described thoroughly.[16,18] Briefly, fentanyl (60 μg/kg, Yichang Humanwell Pharmaceutical co.,ltd, Yichang, China) was injected subcutaneously into the rats every 15 min four times with a cumulative dose of 240 μg/kg to induce OIH. Control rats received an identical volume of 0.9% saline solution. A successful OIH model was confirmed at 6.5 h by a nociceptive behavioral assessment. Notably, in the OIH model, intermittent fentanyl injection differs from chronic drug administration, which can also induce opioid tolerance.[19]

Nociceptive Behavioral Assessment

The mechanical paw withdrawal threshold (PWMT) and thermal paw withdrawal latency (PWTL) were measured in the central left hind paw to assess the susceptibility to detrimental stimuli. Following the last administration of fentanyl (time 0), PWMT and PWTL were evaluated at 0, 1, 3, 5, 6.5, 9, and 12 h, and at 1, 2, 3, 4, 5, and 6 days.

Mechanical Nociceptive Threshold Assessment

The mechanical paw withdrawal threshold was measured with the von Frey filaments (North Coast, San Jose, CA, USA) using an "up and down" method.[16] Rats were imprisoned in a clear plastic compartment with a wire mesh floor prior to behavioral testing until motionless. For approximately 15 s, a succession of calibrated fibers with weights ranging from 0.16–26 g were placed vertically on the plantar surface of the left hind paw. A positive response was defined as an explicit paw withdrawal. The interval between the two stimuli was at least 5 min.

Thermal Nociceptive Latency Assessment

The rats were kept in a transparent plexiglass chamber until immobility before the thermal paw withdrawal latency assessment. A laser beam emitted by a radiant heat stimulator (BME-410C, Biomedical Engineering, Borneo Technology co.,ltd, Guangzhou, China) was directed vertically to the center of the left hind paw through a glass-bottom plate. A positive response was defined as an explicit paw withdrawal. Three reaction times were recorded, and the average PWTL value was calculated. The interval between the two tests was at least 5 min, with a 30 s-cut-off time to avoid excessive tissue damage.

Viral Vector Injection

All viral vectors were purchased from the Brain VTA Company (Wuhan, China). For optogenetically activating viral vector: viral titer was 5×10^{12} particles/mL for both the rAAV 2/9-CaMKIIα-hChR2 (H134R)-eYFP-WPRE-hGh pA and rAAV 2/9-CaMKIIα-eYFP-WPRE-hGh pA (control vector). For chemogenetically inhibiting viral vector: viral titer was 5×10^{12} particles/mL for both the rAAV 2/9-CaMKIIα-hM4D (Gi)-mCherry-WPRE-hGh pA and rAAV 2/9-CaMkIIα-mCherry-WPRE-hGh pA (control vector). Using a 10 μL microsyringe (34 gauge, WPI Company, Sarasota, FL, USA), 0.3 μL of viral vector was microinjected stereotaxically into the right PL-mPFC (coordinates: 3.0 mm anterior to bregma; 0.5 mm lateral to midline; depth, 3.2 mm). All infected rats were fed for 3–4 weeks for virus expression to electrophysiological and behavioral experiments.

Optogenetic Fiber Implantation

A fiber optic cannula (core: 200 μm, length: 7.5 mm, Inper Corporation, Hangzhou, China) was implanted into the NAc core (coordinates: 2.0 mm anterior to bregma; 2.2 mm lateral to midline; depth, 7.0 mm) 2–3 weeks after viral injection. Subsequently, each rat was housed individually in a cage to minimize cannula dislodgement and kept under the conditions described above. All rats were left to recover for at least 1 week before optogenetic behavioral experiments were performed.

Optogenetic Behavioral Assessment

A stimulator (Inper Corporation) capable of luminating a 465 nm laser was connected to an optical fiber via a fiber-optic cable. PL-mPFC neuron terminals projecting to the NAc core were activated using laser light pulses (20 Hz, 5 ms, 10 mW) produced by a blue laser for 20 s. During this period, the PWMT and PWTL were independently measured using the aforementioned methods. Light stimulation was spaced at least 5 min apart.

Chemogenetics Cannulation and Microinjection

Rats were annesthetized with ketamine (50 mg/kg) and xylazine (7.5 mg/kg) and fixed on a stereotaxic apparatus (RWD Life Science, Shenzhen, China). A 33-gauge cored cannula was inserted into the right NAc core area (coordinates: 2.0 mm anterior to the bregma; 2.2 mm lateral to the midline; depth, 7.0 mm). The rats were individually raised for at least 1 week to recuperate from cannulation after surgery. Clozapine-N-Oxide (CNO, Brain VTA Company) was dissolved in dimethyl sulfoxide at a concentration of 0.1 mg/L to produce a working solution of 0.5 μM before microinjection into the right NAc core (coordinates: 2.0 mm anterior to the bregma; 2.2 mm lateral to the midline; depth, 7.0 mm). Behavioral tests were carried out as previously described 30–45 min after CNO administration.

Electrophysiology Slice Preparation

The brain tissues of the rats were stored in ice-cold artificial cerebrospinal fluid (ACSF) saturated with a mixture of 95% O_2 and 5% CO_2 for at least 1 hour. The ACSF consists of 2.6 mM $CaCl_2$, 5 mM KCl, 1.2 mM NaH_2PO_4, 1.3 mM $MgCl_2$, 125 mM NaCl, 26 mM $NaHCO_3$, and 10 mM glucoses (PH = 7.3–7.4, osmolality: 290–310 mOsm/L). Coronal brain slices containing the target brain area (300 μm) were prepared via a vibration microtome (Leica, VT1200S, Wetzlar, Germany) and subsequently incubated in a chamber containing aerated ACSF for 30–60 min at 37 °C. Recordings were made at different time points after the virus injection.

Electrophysiology Patch-Clamp Recording

Virus-labeled cells were identified using a Nikon microscope (Nikon, Tokyo, Japan) and activated using blue light (472 nm, 1 Hz). The internal solution containing 145 mM KCl, 10 mM HEPES, 5 mM EGTA, 5 mM NaCl, 4 mM Mg-ATP, and 0.3 mM Na_3GTP (PH = 7.3, osmolality: 295 mOsm/L) was prepared and stored at −20 °C. The electrodes (impedance: 4–6 MΩ) were pulled out with a Flaming/Brown Micropipette Puller (Model P-97, Sutter Instrument, Novato, CA, USA), and filled with the internal solution up to 1/3 of the height of the electrodes. A dual four-pole Bessel filter (Warner Instruments, Hamden, CT, USA), low-noise Digidata 1322 interface (Molecular Devices, Sunnyvale, CA, USA), HEKA EPC-10 amplifier (HEKA, Lambrecht, Germany), Pentium PC, and Patch Master software (Molecular Devices, San Jose, CA, USA) were used for data acquisition and analyses.

For the PL region, we recorded only the virus-labeled pyramidal neurons in layer V. Action potentials of labeled neurons in layer V PL-mPFC were evoked by a series of current steps (ranging from 0–140 pA in 20 pA increments) for 1.2 s at a membrane potential of −70 mV. For the NAc core region, we recorded only the virus-labeled neurons projecting from the PL-mPFC. To record light-evoked excitatory postsynaptic currents (eEPSC) and light-excited inhibitory postsynaptic currents (eIPSC), 5 mM QX-314 (MCE, New Jersey, USA) was added to the internal solution, and blue light stimulation was provided using a 40 × water-immersion objective lens (Eclipse FN1, Nikon) for 2 ms to activate channelrhodopsin-2 (ChR2) (pE-300 white, CoolLED co.,ltd, Andover, UK). eEPSC and eIPSC were recorded in voltage-clamp mode at −70 mV and −30 mV, respectively.

To investigate the connectivity between the PL-mPFC and the NAc core, the eEPSC of the NAc core neurons projected from the PL-mPFC were recorded in voltage-clamp mode at −70 mV. Sections were perfused with tetrodotoxin (TTX, 1 μM, Tocris Bioscience, Minneapolis, MN, USA), and then the potassium channel blocker 4-aminopyridine (4-AP, 100 μM, MCE) was added, and the eEPSC was recorded before and after dosing, respectively.

Histology and Imaging

Rats were deeply anesthetized and perfused with 0.1 M phosphate-buffered saline (PBS, pH 7.4, Sinopharm Chemical Reagent co.,ltd, Shanghai, China) via the left ventricle, followed by continued perfusion with paraformaldehyde (PFA, pH 7.4, Sinopharm Chemical Reagent co.,ltd). The skull was clipped and cut open, and the brain was removed, and fixed in 4% PFA overnight at 4 °C. After serial dehydration in 20% and 30% sucrose solutions, coronal sections (30 μm) were obtained via a Leica vibration microtome and stored in 0.1 M PBS at 4 °C until immunostaining. To verify the viral expression at the target location, brain slices from the PL-mPFC or NAc regions were selected for whole-brain scanning. Confocal images were obtained using a Nikon TE-200 U inverted fluorescence microscope equipped with a 10 × objective lens. Neuronal excitability of PL-mPFC layer V excitatory neurons was assessed by co-staining of cellular oncogene-Finkel–Biskis–Jinkins osteosarcoma (c-Fos) and calcium/calmodulin-dependent protein kinase II α (CaMKIIα). For c-Fos immunostaining, the brain slices were blocked in 24-well tissue culture plates (Biofil, Guangzhou, China) for 10 min at room temperature using QuickBlockTM Immunostaining Blocking Buffer (Beyotime, Shanghai, China). Sections were then incubated with primary antibodies against c-Fos (1:300, rabbit, CST, Danvers, MA, USA) and CaMKIIα (1:300, mouse, CST) at 4 °C for 12 h. After washing with 0.1 M PBS, sections were incubated with fluorophore-coupled secondary antibodies (1:300, Alexa Fluor 488 donkey anti-rabbit lgG (H + L), Cy3 goat anti-mouse IgG (H + L)) for 2–4 h at room temperature. The nucleus was stained with DAPI staining solution (Beyotime) for 10 min. Subsequently, brain sections were washed with 0.1 M PBS three times for 10 min, and finally fixed on microscope slides. Confocal images were captured using a Nikon TE-200 U inverted fluorescence microscope with a 40 × objective lens, and the number of c-Fos-positive cells was calculated using the Image J analysis system (National Institutes of Health, Bethesda, MD, USA).

Statistical Analysis

Two-way analysis of variance (ANOVA) with Bonferroni adjustments was used to analyze behavioral test results. Continuous variables were presented as mean ± standard error of the mean (mean ± SEM) and analyzed by unpaired Student's *t*-test. All statistical analyses were performed using SPSS (version 20.0, SPSS Inc., Chicago, IL, USA) and GraphPad Prism 5.0 (San Diego, CA, USA). A two-tailed P-value < 0.05 was considered statistically significant.

Results

Fentanyl-Induced Mechanical and Thermal Hyperalgesia in Rats Was Most Pronounced at 6.5 h

To conform to our subsequent behavioral and electrophysiological tests, we selected male Sprague-Dawley rats weighing 200–280 g for subcutaneous injection of fentanyl to induce OIH. Figure 1A shows a schematic diagram of the experimental design. The mechanical and thermal pain thresholds of OIH rats significantly increased within 1 hour after administering the last fentanyl injection (Figure 1B and C), which could be explained by the acute analgesic effect of the opioid drug. Both mechanical and thermal pain thresholds reached their lowest point at 6.5 h after fentanyl administration. The pain sensation lasted for 3–4 days, and then gradually returned to normal on 5–6 days. These results are consistent with those of previous researches.[15,20]

Intrinsic Excitability of the PL-mPFC Layer V Output Neurons Was Decreased in OIH Rats

Immunofluorescence and electrophysiological methods were used to demonstrate changes in the excitability of PL-mPFC layer V output neurons in the OIH state. Figure 2A shows a schematic representation of the immunofluorescence

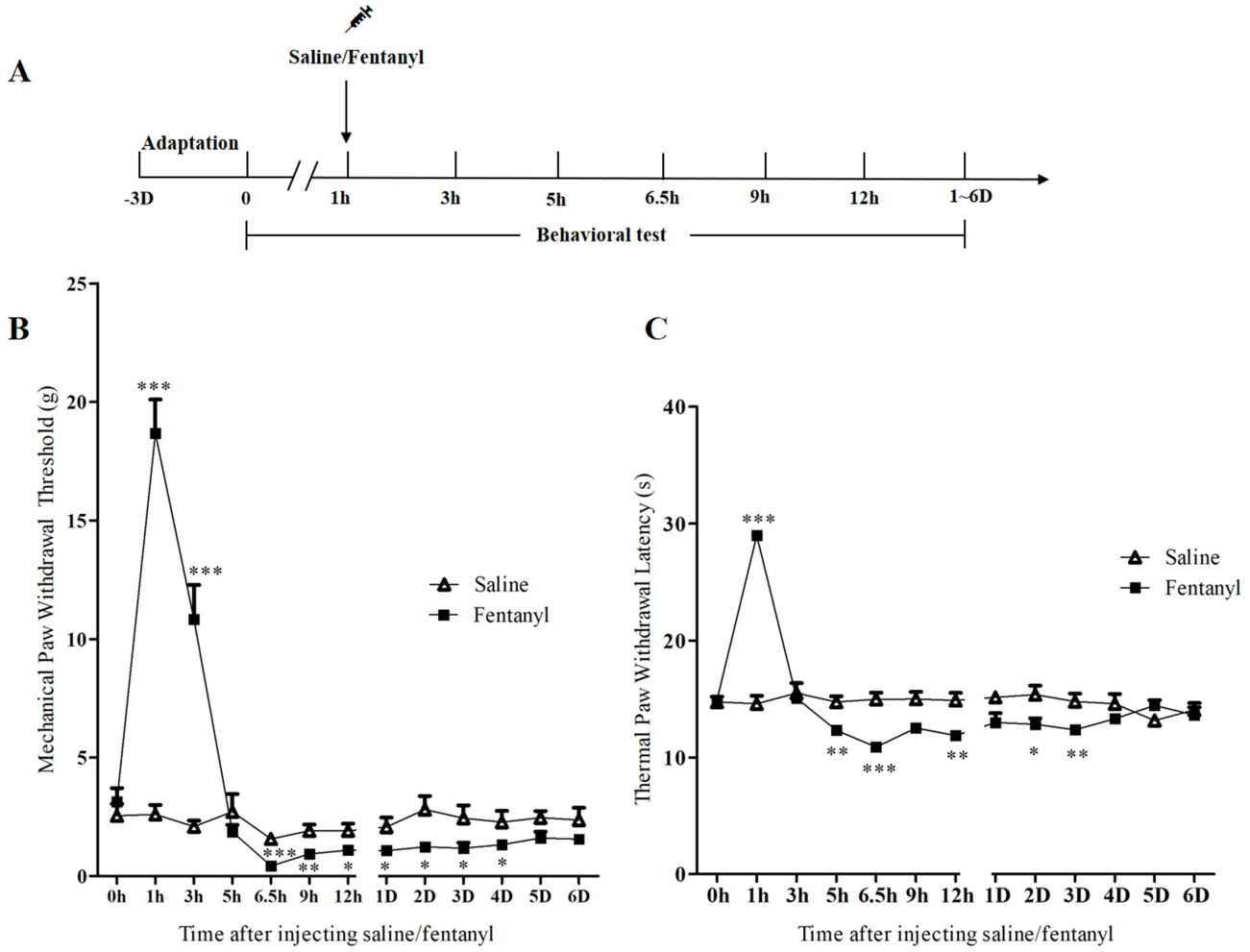

Figure 1 Time history of behavioral hyperalgesia onset in the control (saline-treated) and OIH (fentanyl-treated) groups. (**A**) The conceptual design of the behavioral experiments. (**B**) Time course of the mechanical paw withdrawal threshold in both control and OIH groups (two-way ANOVA; F (Drug 1, 10) = 17.26, $P < 0.01$; F (Time 12, 120) = 45.60, $P < 0.001$; F (Interaction 12, 81) = 42.91, $P < 0.001$; n = 8). (**C**) Time course of the thermal paw withdrawal latency in the control and OIH groups (two-way ANOVA; F (Drug 1, 10) = 3.916, $P < 0.05$; F (Time 12, 120) = 35.21, $P < 0.001$; F (Interaction 12, 81) = 39.46, $P < 0.001$; n = 8). *$P < 0.05$, **$P < 0.01$, ***$P < 0.001$.

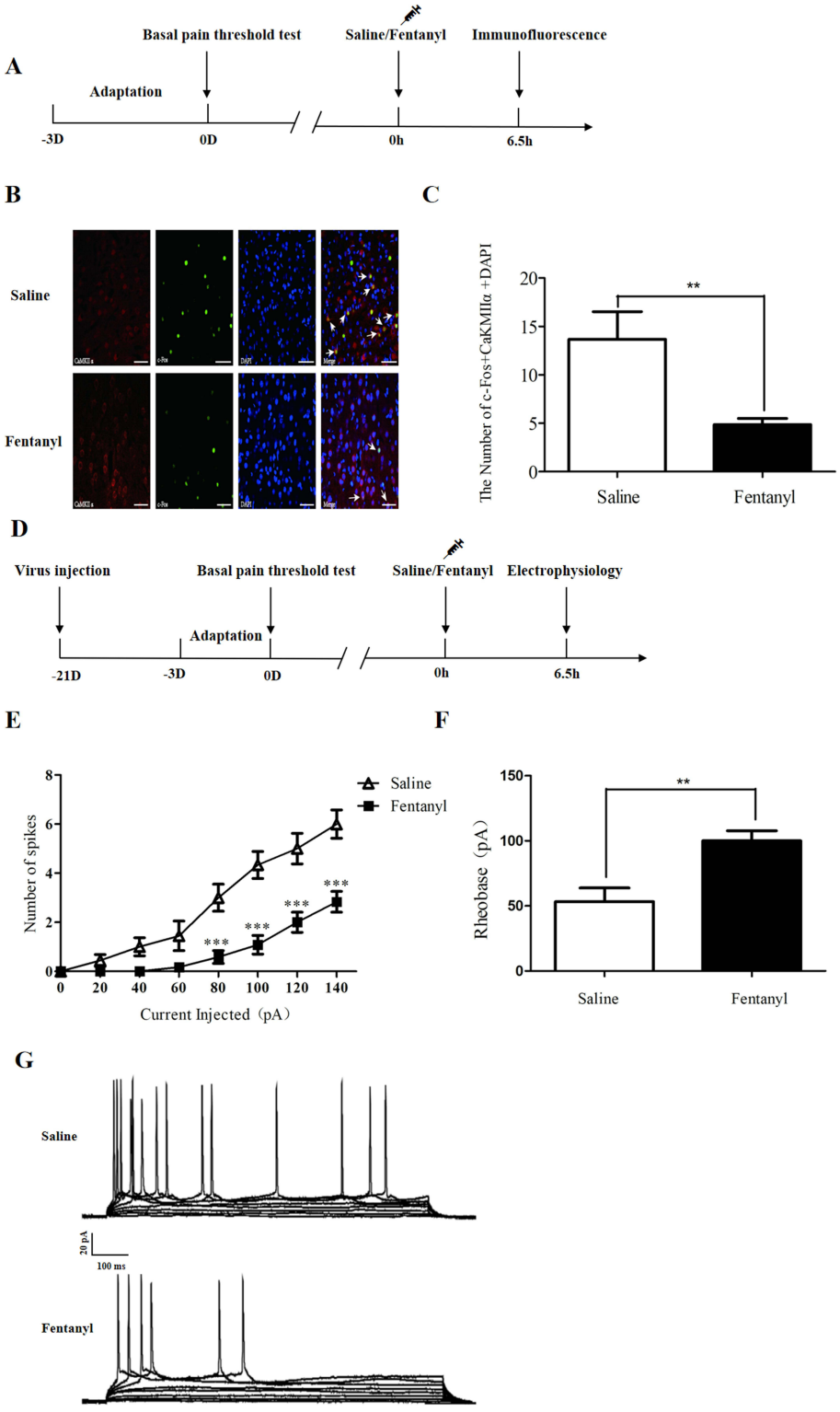

Figure 2 Excitability analysis of the PL-mPFC layer V output neurons in OIH state. (**A**) The schematic diagram of the immunofluorescence experimental design. (**B**) The immunofluorescent co-staining of CaMKIIα (a presumed glutamatergic neuron marker) and c-Fos (a representative neuronal excitability marker). The colors displayed are as follows: CaMKIIα in red, c-Fos in green, and DAPI in blue (scale bar: 50 μm). The co-labeled cells are shown by white arrows. (**C**) The quantitative results of co-staining cells in the saline and fentanyl-treated groups (unpaired *t*-test; $P < 0.01$, n = 6). (**D**) The schematic diagram of the electrophysiological experimental design. (**E**) Plot of the number of spikes responding to different intensities of depolarizing current steps (0–140 pA, 1.2 s) for neurons in the saline and fentanyl-treated groups (two-way ANOVA; F (Drug 1, 152) = 97.83, $P < 0.001$; F (Current steps 7, 152) = 39.99, $P < 0.001$; F (Interaction 7, 152) = 6.215, $P < 0.001$; n = 8). (**F**) The rheobase, defined as the minimal current required to trigger an action potential, was recorded in the control and OIH groups (unpaired *t*-test; $P < 0.01$, n = 8). (**G**) Representative trajectory plot of action potential in the control and OIH groups. $^{**}P < 0.01$, $^{***}P < 0.001$.

experimental design. The number of cells co-expressing the c-Fos and CaMKIIα (a putative marker of glutamatergic neurons) was calculated to determine the excitability of the PL-mPFC layer V output neurons. White arrows indicate co-labeled cells. Figure 2B and C shows that the number of co-labeled cells decreased in OIH rats more than in the control rats. Figure 2D shows a schematic representation of the electrophysiological experimental design. Only virus-labeled cells in layer V were recorded and analyzed. In OIH rats, the reduction in the excitability of PL-mPFC layer V output neurons was observed by a decrease in the number of spikes representing action potentials and an increase in the rheobase (Figure 2E and F). Figure 2G shows the representative action potential trajectories of the two groups. These results suggested that the excitability of PL-mPFC layer V output neurons was decreased in OIH rats than in the control group.

Glutamatergic Projection from the PL-mPFC to the NAc Core Was Predominantly Monosynaptic

PFC-NAc projections are crucial for the reward circuit of the brain. Moreover, chronic opioid usage can induce transcriptional alterations in PFC and NAc.[21] Therefore, we investigated the synaptic connections between PL-mPFC and NAc and the regulatory role of the PL-NAc core in OIH. Figure 3A shows a schematic diagram of the experimental design. Figure 3B shows the glutamatergic projections from the PL-mPFC to the NAc core. To verify the connectivity between the PL-mPFC and NAc core, we microinjected AAV-CaMKIIα-ChR2-eYFP virus into the right PL-mPFC, and 3–4 weeks later, brain slices containing PL-mPFC and NAc core area were obtained for subsequent electrophysiological experiments. Virus-labeled neurons in the brain slices containing the PL-mPFC were fully activated by blue light pulse stimulation, demonstrating ChR2 expression in these neurons (Figure 3C). Whole-cell recordings were made in brain slices containing the NAc core by selecting PL-mPFC neuron terminals projecting to the neurons in the NAc core. The eEPSC in the NAc core region was recorded by stimulating PL-mPFC terminals with blue light (473 nm, 1 ms), which clamped the membrane potential at −70 mV, followed by the addition of TTX and 4-AP in the recording chamber, which resulted in the disappearance and recovery of eEPSC, respectively (Figure 3D and E). These results indicate that the glutamatergic projection from the PL-mPFC to the NAc core was predominantly monosynaptic, which is consistent with the conclusions of previous research.[22]

Excitability of the NAc Core Neurons Receiving Glutamatergic Projection from the PL-mPFC Was Decreased in OIH Rats

Neurons in the NAc core projecting from the PL-mPFC neuron terminals were stimulated using a blue laser (473 nm, 1 ms), and eEPSC and eIPSC were recorded (Figure 4A). Our results showed that the eEPSC and eIPSC amplitudes decreased and increased, respectively, in the fentanyl-induced OIH group compared with those in the saline-treated control group (Figure 4B and C), which resulted in a lower eEPSC/eIPSC ratio, representing a weaker synaptic connection in OIH rats (Figure 4D). In addition, the number of action potential spikes decreased, and the rheobase of the threshold action potential increased in the OIH group, demonstrating the reduced excitability of neurons projecting from the PL-mPFC toward the NAc core region (Figure 4E and F). Therefore, hyperalgesia caused by repeated acute fentanyl injections is associated with reduced excitability of neurons projected from the PL-mPFC toward the NAc core.

Optogenetic Activation of the PL-NAc Core Pathway Reversed Fentanyl-Induced Hyperalgesia

We observed the behavioral alterations in rats before and after light activation using in vivo optogenetic techniques. Figure 5A shows an experimental schematic of optogenetics. Rats were microinjected with the rAAV2/9-CaMKIIα-hChR2 (H134R)-eYFP -WPRE-hGh pA (AAV-CaMKIIα-hChR2 group) and rAAV2/9-CaMKIIα-eYFP-WPRE-hGh pA (AAV-CaMKIIα group) viral vectors. 2 weeks later, fiber optic cannula was implanted into the right NAc core. Baseline mechanical and thermal thresholds were examined 3 weeks after virus expression onset. Rats injected with AAV-CaMKIIα-hChR2 and AAV-CaMKIIα were divided into saline-treated control and fentanyl-treated OIH groups. Behavioral tests were assessed 6.5 h after OIH modeling. As shown in Figure 5B and C, light activation of the PL-NAc core pathway reversed the decreased mechanical and thermal pain thresholds caused by fentanyl administration in the AAV-CaMKIIα-hChR2 group, whereas no statistical difference in the

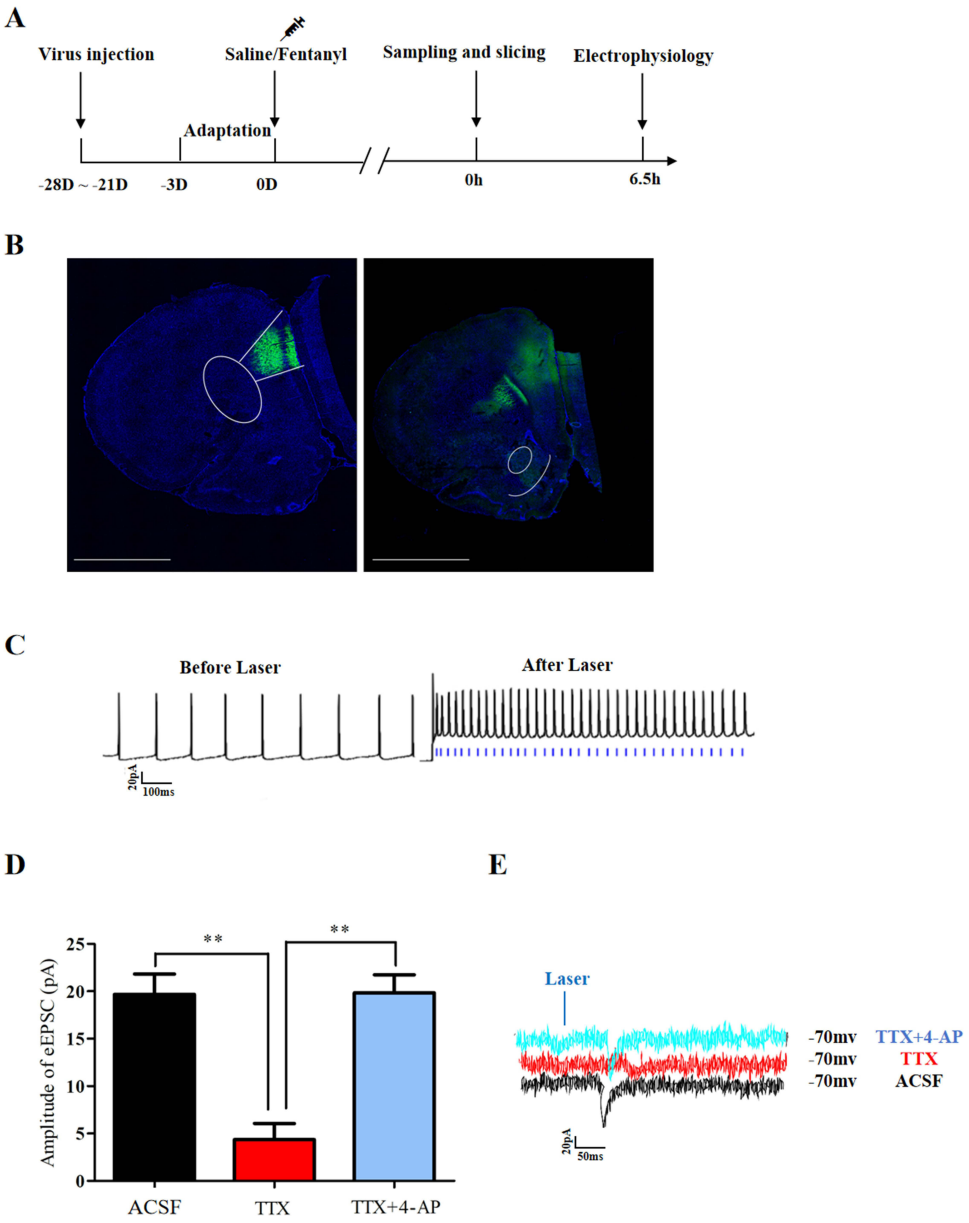

Figure 3 Synaptic linkage analysis between the PL-mPFC and the NAc core. (**A**) The schematic diagram of the electrophysiological experimental design. (**B**) The schematic representation of the viral injection site in the PL-mPFC (left) and PL-NAc virus projection (right) (scale bar: 1000 μm). (**C**) Action potentials were recorded in neurons expressing ChR2-eYFP in the PL-mPFC in current-clamp mode (blue light: 465 nm, 43.7 mW, 5 ms duration) at 5 Hz in order to identify the virus function (blue vertical lines represent light stimulation pulses). (**D**) The eEPSC was recorded in each group. The eEPSC was completely blocked by TTX (1 μM) and recovered by consequent 4-AP (100 μM) (ACSF vs TTX: $P < 0.01$; TTX vs TTX + 4-AP: $P < 0.01$). (**E**) The typical eEPSC trajectory diagrams of three groups. The colors displayed are as follows: ACSF group in black, TTX group in red, and TTX + 4-AP group in blue. $^{**}P < 0.01$.

behavioral performance caused by fentanyl administration before and after light activation of the PL-NAc core pathway was observed in the AAV-CaMKIIα group. These results suggest that the optogenetic activation of the PL-NAc core pathway reverses fentanyl-induced hyperalgesia.

Chemogenetic Inhibition of the PL-NAc Core Pathway Induced Hyperalgesia in Saline-Treated Rats

As activation of the PL-NAc core pathway reversed fentanyl-induced hyperalgesia, we hypothesized that inhibition of this pathway could induce hyperalgesia in control rats or worsen the OIH state. Figure 6A shows an experimental

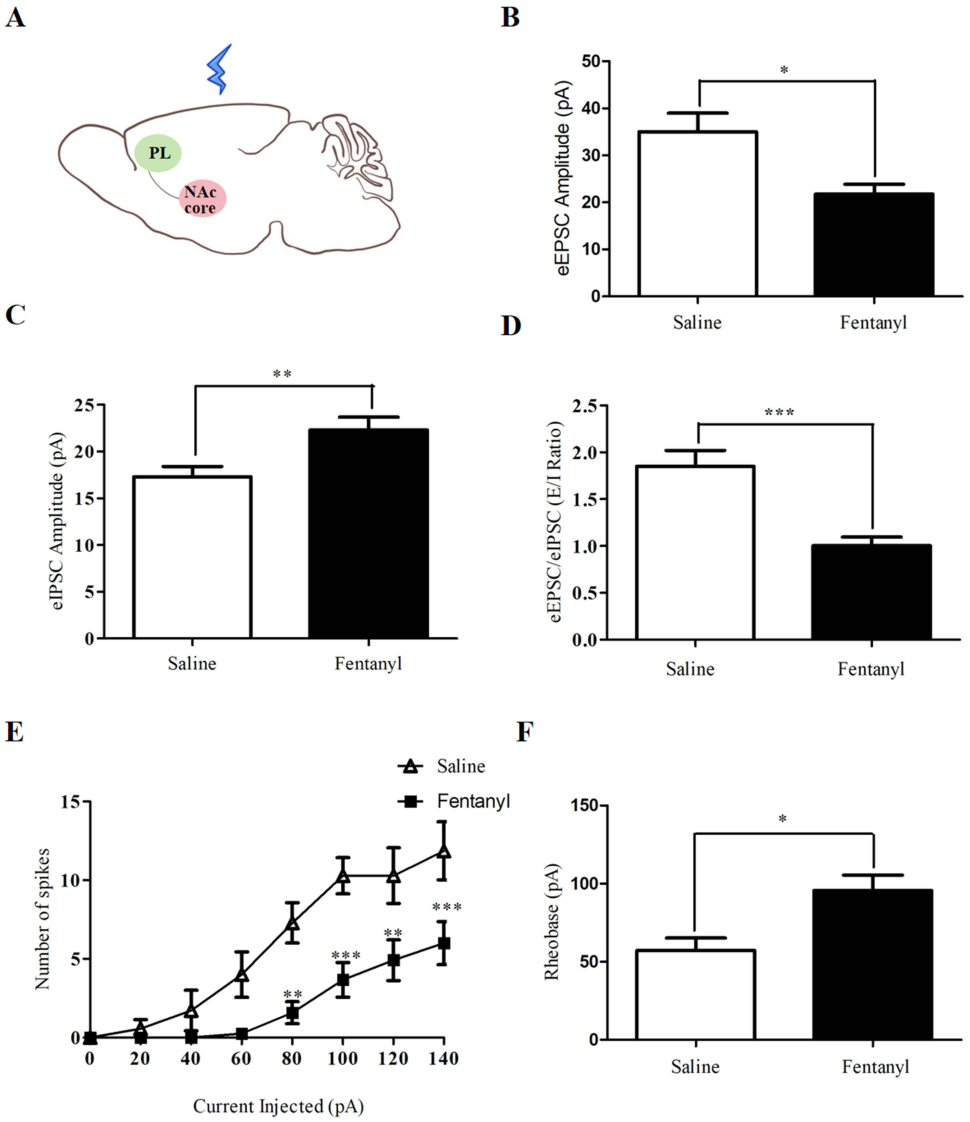

Figure 4 Excitability assay of neurons projected from the PL-mPFC toward the NAc core. (**A**) The schematic diagram represents the recording of eEPSC and eIPSC in the PL-NAc region. (**B**) The quantitative results of the eEPSC amplitude in the control and OIH groups (unpaired *t*-test; $P < 0.05$, n = 22 in control, n = 18 in OIH). (**C**) The quantitative results of the eIPSC amplitude in the control and OIH groups (unpaired *t*-test; $P < 0.01$, n = 22 in control, n = 18 in OIH). (**D**) The eEPSC/eIPSC ratio in the control and OIH groups (unpaired *t*-test; $P < 0.001$). (**E**) Plot of the number of spikes responding to different intensities of depolarizing currents (0–140 pA, 1.2 s) for the NAc core neurons in the control and OIH groups (two-way ANOVA; F (Drug 1, 48) = 52.08, $P < 0.001$; F (Current steps 7, 88) = 24.16, $P < 0.001$; F (Interaction 7, 48) = 3.223, $P < 0.01$; n = 22). (**F**) Minimum rheobase for the excitation of an action potential from the NAc core in the control and OIH groups (unpaired *t*-test; $P < 0.05$, n = 9). *$P < 0.05$, **$P < 0.01$, ***$P < 0.001$.

schematic of the chemogenetics. The rAAV2/9-CaMKIIα-hM4D (Gi)-mCherry-WPRE-hGh pA (hM4D-mCherry group) and rAAV2/9-CaMkIIα-mCherry-WPRE-hGh pA (mCherry group) viral vectors were microinjected into the right PL-mPFC of rats. Two weeks after the virus injection, the cannula was implanted into the right NAc core. Baseline mechanical and thermal thresholds were examined 3 weeks after virus expression onset. Rats injected with hM4D-mCherry and mCherry were then divided into saline-treated control and fentanyl-treated OIH groups, and behavioral tests were assessed 6.5 h after OIH modeling. Whole-cell patch-clamp recordings of the PL-mPFC slices from human muscarinic 4 receptor-based GI-coupled DREADD (hM4D)-expressing rats revealed that CNO drastically reduced neuronal activity in virus-transfected cells (Figure 6B), demonstrating that hM4D and CNO did function to suppress cell excitability. Rats injected with mCherry (control vector) showed no statistical difference in the mechanical and thermal pain thresholds before and after CNO microinjection in both the saline- and fentanyl-treated groups (Figure 6C

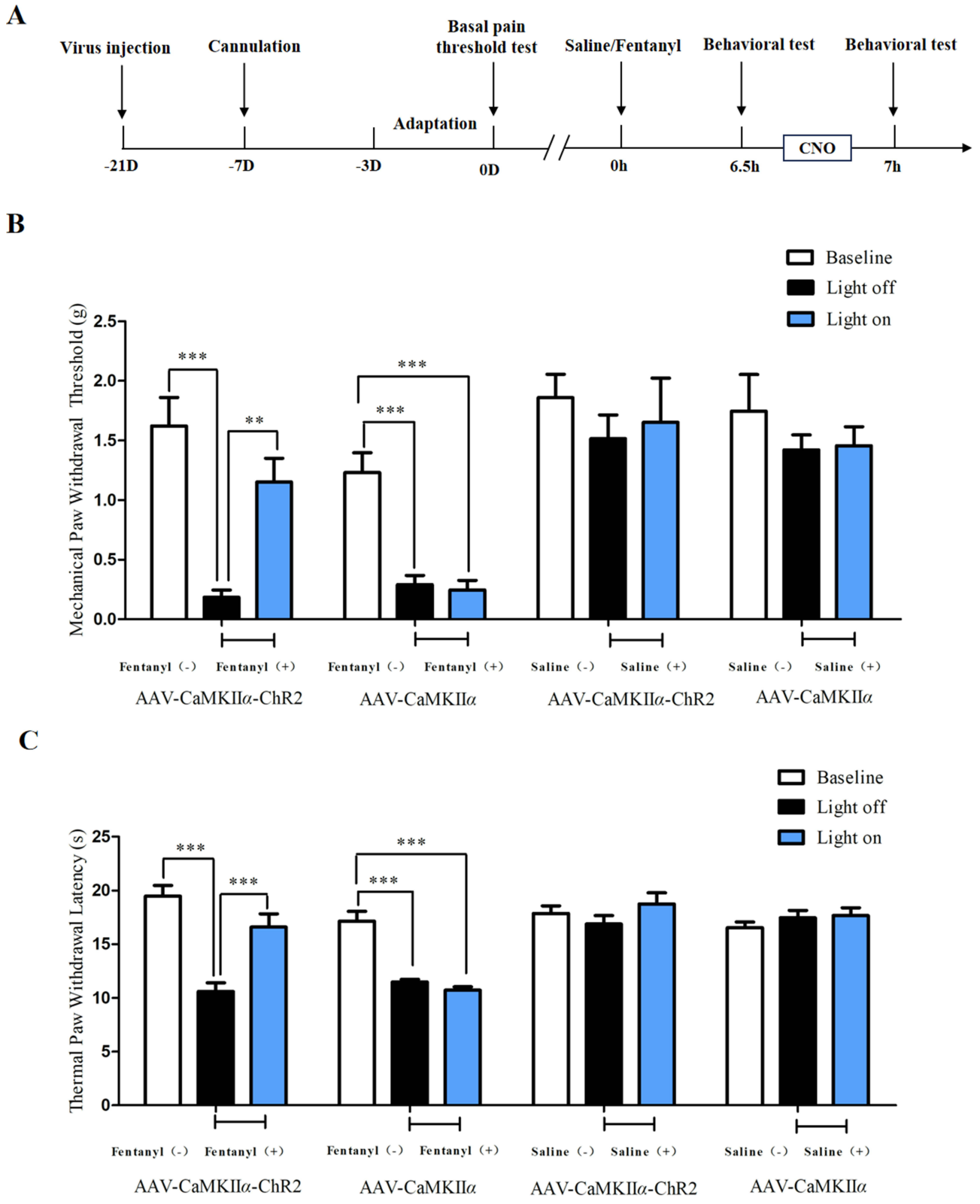

Figure 5 Behavioral performance in rats before and after optogenetic activation. (**A**) The schematic diagram of optogenetic behavior experiments. (**B**) The mechanical paw withdrawal threshold in each group before and after light activation of the PL-NAc core pathway (light off vs light on: $P < 0.01$ in fentanyl-treated AAV-CaMKIIα-ChR2 group, n = 4). (**C**) The thermal paw withdrawal latency in each group before and after light activation of the PL-NAc core pathway (light off vs light on: $P < 0.001$ in fentanyl-treated AAV-CaMKIIα-ChR2 group, n = 4). *$P < 0.05$, **$P < 0.01$, ***$P < 0.001$.

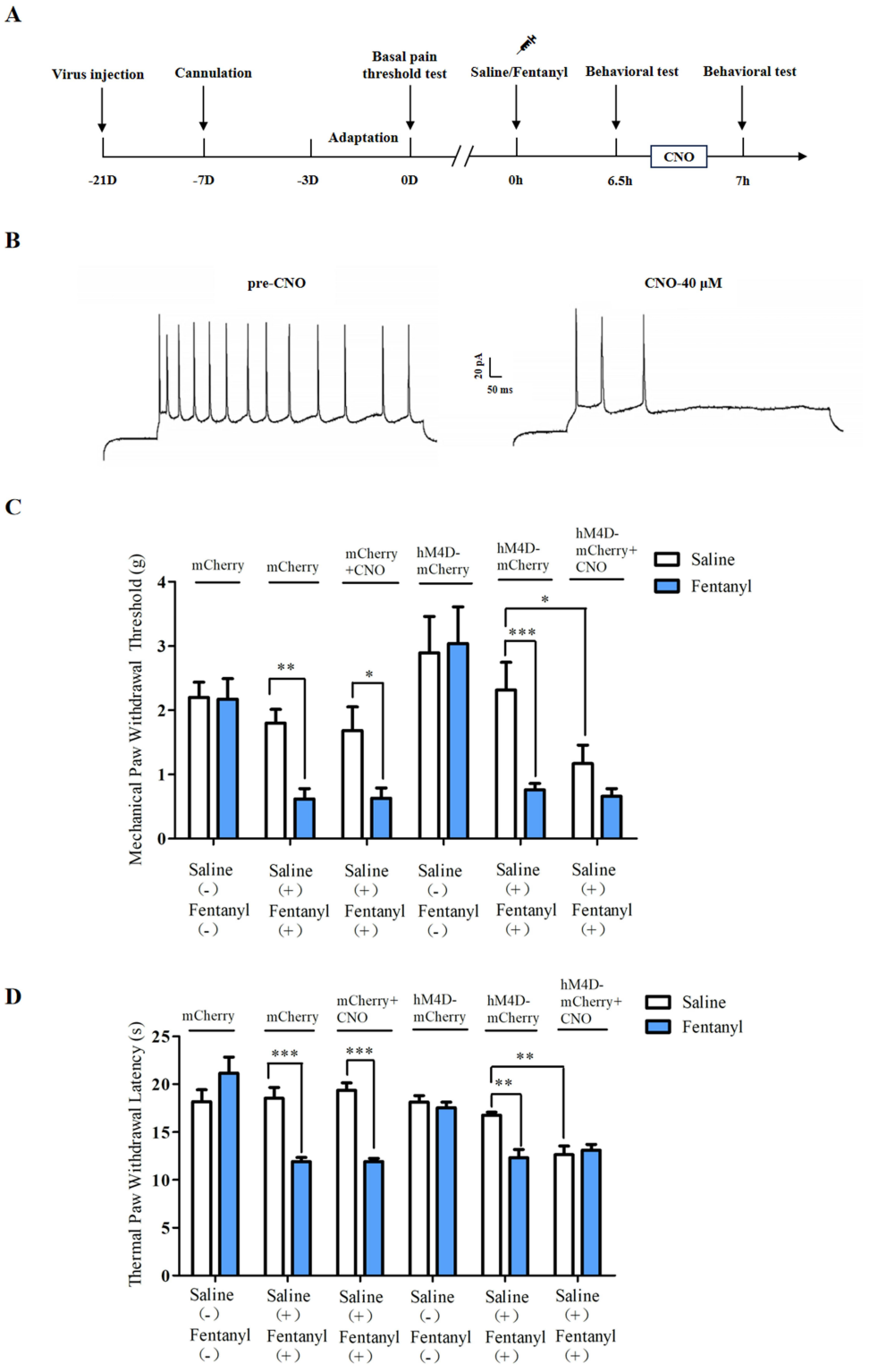

Figure 6 Behavioral performance in rats before and after chemogenetic inhibition. (**A**) The experimental schematic diagram of chemogenetics. (**B**) Action potentials of hM4D-mCherry-expressing neurons in the PL-mPFC were recorded in current-clamp mode before and after CNO (40 μM) incubation. (**C**) The mechanical paw withdrawal threshold in each group before and after CNO (0.5 μM, 0.5 μL) injection (unpaired *t*-test; mCherry vs mCherry + CNO: $P > 0.05$ in saline-treated group, n = 4; hM4D-mCherry vs hM4D-mCherry + CNO: $P < 0.05$ in saline-treated group, n = 4). (**D**) The thermal paw withdrawal latency in each group before and after CNO injection (unpaired *t*-test; mCherry vs mCherry + CNO: $P > 0.05$ in saline-treated group, n = 4; hM4D-mCherry vs hM4D-mCherry + CNO: $P < 0.01$ in saline-treated group, n = 4). *$P < 0.05$, **$P < 0.01$, ***$P < 0.001$.

and D). In rats injected with hM4D-mCherry, no significant difference in pain thresholds before and after CNO microinjection in the fentanyl-treated group was observed. However, pain thresholds decreased in the saline-treated group after receiving CNO. These results suggest that inactivation of the PL-NAc core pathway aggravates hyperalgesia in control rats but not in OIH rats.

Discussion

Our results showed that the pain thresholds were the lowest at 6.5 h after fentanyl administration, which is consistent with the findings of a previous study.[15] Therefore, follow-up experiments were conducted using this time point. In this study, we first evaluated the intrinsic excitability of PL-mPFC pyramidal neurons in layer V of an OIH model using electrophysiological and immunofluorescence methods. The results showed that the excitability of glutamatergic neurons in layer V of the PL-mPFC was decreased in OIH rats, observed by a reduction in the number of action potential firings and an increase in the rheobase to ignite action potentials. Similarly, the number of cells co-labeled with c-Fos and CaMKIIα in layer V of the PL-mPFC was decreased in OIH rats. We focused on the PL-NAc core glutamatergic circuit and investigated its role in OIH. Optogenetic and electrophysiological results suggested that the excitability of the NAc core neurons receiving glutamatergic projections from the PL-mPFC decreased in OIH rats, observed by a lower eEPSC/eIPSC ratio, reduced number of action potential firings, and increased rheobase. In addition, optogenetic activation of the PL-NAc core pathway reversed fentanyl-induced hyperalgesia, whereas chemogenetic inhibition of the PL-NAc core pathway induced hyperalgesia in control rats. However, in OIH rats, behavioral hyperalgesia was not aggravated by this inhibition, suggesting that reduced activity of the PL-NAc core pathway was most likely the initiating cause of OIH. Therefore, we identified a novel brain circuit for OIH regulation.

The prelimbic cortex, a subregion of the mPFC, contributes to the comorbidity of neuropathic pain and depression.[13] Inhibition of oligodendrocyte apoptosis in the PL-mPFC could prevent fentanyl-induced hyperalgesia in rats.[15] These findings demonstrate that the PL-mPFC subregion is closely related to pain processes. Additionally reduced activity of output neurons (mainly pyramidal cells) in the PL-mPFC has been demonstrated in rodent models of inflammatory and neuropathic pain,[23,24] and a possible explanation is the abnormally increased glutamatergic activation of parvalbumin-expressing GABAergic (gamma-aminobutyric acidergic) interneurons.[24,25] Furthermore, Cdk5 signaling is a potential mechanism molecule responsible for the changes of the PL excitatory neurons in pain regulation.[23] Moreover, an inverse interaction between infralimbic and prelimbic mPFC regions exists,[26] activation of the IL output can inhibit the PL pyramidal cells. Therefore, further research is needed to evaluate the change of excitability in the IL-mPFC region in OIH.

Generally, the PL-mPFC modulates pain through projections to several other brain regions, including the amygdala, NAc, and the PAG.[27] Among them, the NAc is important in sensory and emotional pain responses.[9] The principal cells in the NAc are a group of GABAergic projection medium-spiny neurons (MSNs) that express either dopamine D1 or D2 receptor (D1R or D2R), and have specialized functions in NAc-mediated behaviors and illnesses.[22] Current research shows that the involvement of the NAc core in pain regulation is mostly related to the D2R, observed by the combination of reduced D2R expression and signaling in the NAc core in an intraplantar (Ipl) formalin model of chronic pain.[28] In addition, inhibition of dopaminergic signaling in the NAc core alters the intrinsic excitability and synaptic connectivity of D2R-expressing spiny projection neurons.[29] However, whether D2R in the NAc core of glutamatergic PL-mPFC functions in the OIH state remains unclear and warrants further investigation.

Studies have reported the regulatory roles of PL-mPFC and NAc in OIH, however, it is unclear whether the PL-NAc pathway is altered in OIH.[15,30] In fact, mPFC-NAc projections manage pain, and activation of the mPFC-NAc pathway can help alleviate chronic pain.[9,14] Considering our findings on the PL-mPFC circuit involved in OIH and the additional refined projection characteristics of the PL-mPFC to the NAc region, as previously described,[14,15] we focused on the PL-NAc core pathway and aimed to explore its role in OIH. Based on the electrophysiological results showing that the excitatory transmission from the PL-mPFC to the NAc core decreased and inhibitory transmission increased in the OIH state, we speculate that the EPSC/IPSC ratio imbalance may be a crucial mechanism of the NAc core inactivity. Descending modulation of the spinal dorsal horn via the PAG-RVM circuit controls central pain,[31] and both the PAG and the brainstem receive signals from the NAc.[32] Thus, it is reasonable that corticostriatal projections produce descending pain suppression via the PAG-RVM pathway. Taken together, our results demonstrate that the PL-NAc core circuit is involved in the development of OIH and that restoring the activity of the prefrontal cortex to the NAc core pathway could relieve fentanyl-induced hyperalgesia in male rats.

Despite the growing recognition of gender variations in pain sensitivity, the trials reported here are conducted only on male rats, as in our and most other earlier studies.[16,17,20] As shown in previous research, there are significant sex differences in the cortical and subcortical processing of pain.[33–35] It must be noted that we did not study how the PL-mPFC alone regulates OIH or whether it is regulated by the NAc feedback. Future functional mapping of various microcircuits within corticostriatal projections is essential for determining the regulatory mechanism of the striatum and cortex in OIH.

Conclusion

In summary, we identified a new circuit that modulates OIH and demonstrated that the PL-NAc core pathway plays a crucial role in fentanyl-induced hyperalgesia. Restoring the PL-NAc core pathway activity alleviated OIH. Additionally, inhibiting the PL-NAc core pathway induced nociceptive hypersensitivity in the control group but not in the OIH group, suggesting that inactivation of the PL-NAc core pathway may cause OIH. Therefore, exploiting the PL-NAc core pathway activity may provide strategies for OIH treatment in the future.

Data Sharing Statement

The data used to support the results of this study can be obtained from the corresponding author upon reasonable request.

Ethics Approval and Informed Consent

This study was performed in accordance with the ethical guidelines of the Laboratory Animal and Biomedical Ethics Committee of the South-Central University for Nationalities (Number: 2019- SCUEC-AEC-022).

Acknowledgments

The study was undertaken in the laboratory of Prof. Chenhong Li at the South-Central University for Nationalities. We sincerely appreciate the animal and electrophysiological experimental platform provided by the South-Central University for Nationalities. We thank the Editage (www.editage.cn) for English language editing.

Funding

This study was supported by grants from the National Natural Science Foundation of China (grant number: 81974165); the Fundamental Research Funds for the Central Universities (grant number: 2042023kf0070).

Disclosure

The authors report no conflicts of interest in this work.

References

1. Sampaio-Cunha TJ, Martins I. Knowing the enemy is halfway towards victory: a scoping review on opioid-induced hyperalgesia. *J Clin Med*. 2022;11(20):6161. doi:10.3390/jcm11206161
2. Wilson SH, Hellman KM, James D, et al. Mechanisms, diagnosis, prevention and management of perioperative opioid-induced hyperalgesia. *Pain Manag*. 2021;11(4):405–417. doi:10.2217/pmt-2020-0105
3. Ossipov MH, Morimura K, Porreca F. Descending pain modulation and chronification of pain. *Curr Opin Support Palliat Care*. 2014;8(2):143–151. doi:10.1097/SPC.0000000000000055
4. Morgan MM, Gold MS, Liebeskind JC, et al. Periaqueductal gray stimulation produces a spinally mediated, opioid antinociception for the inflamed hindpaw of the rat. *Brain Res*. 1991;545(1–2):17–23. doi:10.1016/00068993(91)91264-2
5. Morgan MM, Sohn JH, Liebeskind JC. Stimulation of the periaqueductal gray matter inhibits nociception at the supraspinal as well as spinal level. *Brain Res*. 1989;502(1):61–66. doi:10.1016/0006-8993(89)90461-7
6. Mecca CM, Chao D, Yu G, et al. Dynamic change of endocannabinoid signaling in the medial prefrontal cortex controls the development of depression after neuropathic pain. *J Neurosci*. 2021;41(35):7492–7508. doi:10.1523/JNEUROSCI.3135-20.2021
7. Huang J, Gadotti VM, Chen L, et al. A neuronal circuit for activating descending modulation of neuropathic pain. *Nat Neurosci*. 2019;22 (10):1659–1668. doi:10.1038/s41593-019-0481-5
8. Yu X, Abdul M, Fan BQ, et al. The release of exosomes in the medial prefrontal cortex and nucleus accumbens brain regions of chronic constriction injury (CCI) model mice could elevate the pain sensation. *Neurosci Lett*. 2020;723:134774. doi:10.1016/j.neulet.2020.134774
9. Zhou H, Martinez E, Lin HH, et al. Inhibition of the prefrontal projection to the nucleus accumbens enhances pain sensitivity and affect. *Front Cell Neurosci*. 2018;12:240. doi:10.3389/fncel.2018.00240
10. Vachon-Presseau E, Tetreault P, Petre B, et al. Corticolimbic anatomical characteristics predetermine risk for chronic pain. *Brain*. 2016;139(Pt 7):1958–1970. doi:10.1093/brain/aww100

11. Martinez E, Lin HH, Zhou H, et al. Corticostriatal regulation of acute pain. *Front Cell Neurosci*. 2017;11:146. doi:10.3389/fncel.2017.00146
12. Kummer KK, Mitric M, Kalpachidou T, et al. The medial prefrontal cortex as a central hub for mental comorbidities associated with chronic pain. *Int J Mol Sci*. 2020;21(10):3440. doi:10.3390/ijms21103440
13. Zhao YT, Deng J, Liu HM, et al. Adaptation of prelimbic cortex mediated by IL-6/STAT3/Acp5 pathway contributes to the comorbidity of neuropathic pain and depression in rats. *J Neuroinflammation*. 2022;19(1):144. doi:10.1186/s12974-022-02503-0
14. Lee M, Manders TR, Eberle SE, et al. Activation of corticostriatal circuitry relieves chronic neuropathic pain. *J Neurosci*. 2015;35(13):5247–5259. doi:10.1523/JNEUROSCI.3494-14.2015
15. Wang XX, Cui LL, Gan SF, et al. Inhibition of oligodendrocyte apoptosis in the prelimbic medial prefrontal cortex prevents fentanyl-induced hyperalgesia in rats. *J Pain*. 2022;23(6):1035–1050. doi:10.1016/j.jpain.2021.12.012
16. Wang XX, Gan SF, Zhang ZR, et al. HCN-channel-dependent hyperexcitability of the layer V pyramidal neurons in IL-mPFC contributes to fentanyl-induced hyperalgesia in male rats. *Mol Neurobiol*. 2023;60(5):2553–2571. doi:10.1007/s12035-023-03218-w
17. Li Z, Yin PP, Chen J, et al. CaMKIIalpha may modulate fentanyl-induced hyperalgesia via a CeLC-PAG-RVM-spinal cord descending facilitative pain pathway in rats. *PLoS One*. 2017;12(5):e0177412. doi:10.1371/journal.pone.0177412
18. Celerier E, Rivat C, Jun Y, et al. Long-lasting hyperalgesia induced by fentanyl in rats: preventive effect of ketamine. *Anesthesiology*. 2000;92(2):465–472. doi:10.1097/00000542-200002000-00029
19. Zissen MH, Zhang G, McKelvy A, et al. Tolerance, opioid-induced allodynia and withdrawal associated allodynia in infant and young rats. *Neuroscience*. 2007;144(1):247–262. doi:10.1016/j.neuroscience.2006.08.078
20. Li Z, Li CH, Yin PP, et al. Inhibition of CaMKIIalpha in the central nucleus of amygdala attenuates fentanyl-induced hyperalgesia in rats. *J Pharmacol Exp Ther*. 2016;359(1):82–89. doi:10.1124/jpet.116.233817
21. Seney ML, Kim SM, Glausier JR, et al. Transcriptional alterations in dorsolateral prefrontal cortex and nucleus accumbens implicate neuroinflammation and synaptic remodeling in opioid use disorder. *Biol Psychiatry*. 2021;90(8):550–562. doi:10.1016/j.biopsych.2021.06.007
22. Deroche MA, Lassalle O, Castell L, et al. Cell-type- and endocannabinoid-specific synapse connectivity in the adult nucleus accumbens core. *J Neurosci*. 2020;40(5):1028–1041. doi:10.1523/JNEUROSCI.1100-19.2019
23. Wang GQ, Cen C, Li C, et al. Deactivation of excitatory neurons in the prelimbic cortex via cdk5 promotes pain sensation and anxiety. *Nat Commun*. 2015;6(1):7660. doi:10.1038/ncomms8660
24. Zhang ZZ, Gadotti VM, Chen LN, et al. Role of prelimbic GABAergic circuits in sensory and emotional aspects of neuropathic pain. *Cell Rep*. 2015;12(5):752–759. doi:10.1016/j.celrep.2015.07.001
25. Ji GC, Neugebauer V. Pain-related deactivation of medial prefrontal cortical neurons involves mGluR1 and GABA(A) receptors. *J Neurophysiol*. 2011;106(5):2642–2652. doi:10.1152/jn.00461.2011
26. Ji GC, Neugebauer V. Modulation of medial prefrontal cortical activity using in vivo recordings and optogenetics. *Mol Brain*. 2012;5(1):36. doi:10.1186/1756-6606-5-36
27. Umana IC, Daniele CA, Miller BA, et al. Nicotinic modulation of descending pain control circuitry. *Pain*. 2017;158(10):1938–1950. doi:10.1097/j.pain.0000000000000993
28. Selley DE, Lazenka MF, Sim-Selley LJ, et al. Attenuated dopamine receptor signaling in nucleus accumbens core in a rat model of chemically-induced neuropathy. *Neuropharmacology*. 2020;166:107935. doi:10.1016/j.neuropharm.2020.107935
29. Ren WJ, Centeno MV, Wei XH, et al. Adaptive alterations in the mesoaccumbal network after peripheral nerve injury. *Pain*. 2021;162(3):895–906. doi:10.1097/j.pain.0000000000002092
30. Zhang P, Moye LS, Southey BR, et al. Opioid-induced hyperalgesia is associated with dysregulation of circadian rhythm and adaptive immune pathways in the mouse trigeminal ganglia and nucleus accumbens. *Mol Neurobiol*. 2019;56(12):7929–7949. doi:10.1007/s12035-019-01650-5
31. Palazzo E, Luongo L, Novellis V, et al. The role of cannabinoid receptors in the descending modulation of pain. *Pharmaceuticals*. 2010;3(8):2661–2673. doi:10.3390/ph3082661
32. Guo MM, Wu YX, Zheng DH, et al. Preoperative acute sleep deprivation causes postoperative pain hypersensitivity and abnormal cerebral function. *Neurosci Bull*. 2022;38(12):1491–1507. doi:10.1007/s12264-022-00955-1
33. Jones AF, Sheets PL. Sex-specific disruption of distinct mPFC inhibitory neurons in spared-nerve injury model of neuropathic pain. *Cell Rep*. 2020;31(10):107729. doi:10.1016/j.celrep.2020.107729
34. Gadotti VM, Zhang ZZ, Huang JT, et al. Analgesic effects of optogenetic inhibition of basolateral amygdala inputs into the prefrontal cortex in nerve injured female mice. *Mol Brain*. 2019;12(1):105. doi:10.1186/s13041-019-0529-1
35. Shiers S, Pradhan G, Mwirigi J, et al. Neuropathic pain creates an enduring prefrontal cortex dysfunction corrected by the type II diabetic drug metformin but not by gabapentin. *J Neurosci*. 2018;38(33):7337–7350. doi:10.1523/JNEUROSCI.0713-18.2018